Ultra-low landing energy scanning electron microscopy for nanoengineering applications and metrology*

Michael T. Postek, University of South Florida, Tampa, FL 33612,
András E. Vladár and Dianne L. Poster, National Institute of Standards and Technology, Gaithersburg, MD 20899,
Atsushi Muto and Takeshi Sunaoshi, Hitachi High-Tech America, Clarksburg, MD 20871

ABSRACT

Keywords: scanning electron microscopy, SEM, ultra-low landing energy, nanometrology, nanocoatings, nanogels, nanoparticles

A new and exciting imaging technique being applied to thin films, nanocoatings, nanogels, and nanoparticle analysis is ultra-low accelerating voltage or ultra-low-landing-energy scanning electron microscopy (ULVSEM). Instrument conditions in this mode are different than with typical SEM observation or contemporary low accelerating voltage (LVSEM) imaging. Hence, the images appear far different due to reduced beam penetration. The landing energy of the primary electron beam can be much lower than LVSEM, it can be reduced to far below 500 electron volts (eV), even as low as 10 eV. Thus, the electron beam range and penetration are reduced tremendously with some unavoidable loss of spatial resolution. Surface details are enhanced, contrast might favorably change, and secondary electron (SE) edge enhancement or "blooming" contributing to measurement uncertainty is greatly reduced, potentially allowing for more precise and new measurements once this imaging mode is fully characterized and accurately modeled. High-resolution field-emission electron sources, improved lens, detector designs, and sample biasing all contribute to the ability to image at such low electron landing energies. The techniques of ULVSEM are discussed, and an application example is presented.

1. INTRODUCTION

Scanning electron microscopes (SEM) are used in countless disciplines of scientific, medical, and industrial research. These instruments are also deeply embedded in many manufacturing lines such as semiconductor production. Since its inception in the 1950s, and its introduction as a commercial product in the 1960s, the SEM has gone through continual evolution to become an indispensable tool for its many and diverse applications. The uniqueness of SEM lies within its simplicity – the instrument uses an electron beam source and focuses it into a probe which scans across the surface of a sample in a raster pattern. The resulting electrical interactions are displayed and recorded point-by-point as signal modulation resulting from the scan, hence, the term "scanning" is in the technique's name as an essential term-of-art.

Numerous substantial improvements in capabilities and the ease of operation of the instrument have been made, as this instrument matured. Electron sources have evolved from tungsten hairpin-shaped electron sources to lanthanum hexaboride to cold and thermal field emission, thus providing much higher brightness, better-focused electron beams and improved instrument reliability and performance. This performance has also been enhanced by the incorporation of new innovative electromagnetic and electrostatic lens designs, as well as the replacement of the older analog with highly precise and more complex digital electronics.

High performance is critical for current SEM nanoengineering applications for thin films, nanocoatings, nanogels, and for nanoparticle analysis. This is especially true in the research and production environments which currently heavily rely on the measurement of the collected secondary electron signal data. By definition, secondary electrons are those emitted electrons possessing an energy of 50 eV or less. The SEM was initially introduced as a "surface" imaging tool, as noted

*Contribution of the National Institute of Standards and Technology; not subject to copyright in the United States. Certain commercial equipment, instruments, or materials are identified in this report to specify the experimental procedure adequately. Such identification is not intended to imply recommendation or endorsement by the National Institute of Standards and Technology or the United States Government Publishing Office, nor is it intended to imply that the materials or equipment identified are necessarily the best available for the purpose.

above. As knowledge about the complex physics of electron beam - sample interactions improved, it became clear that, in the SEM, electron beam penetration and signal generation dominate the imaging and analytical performance. In short, electron beam penetration is a function of electron landing energy and atomic number of the target material.[1] Essentially, depending upon operator chosen operating conditions, the actual surface of some samples can be rendered somewhat "transparent" to the electron beam.[2] Then, depending upon the conditions chosen, many of the signals being imaged can originate from deeply in the sample or nearer to the surface with all of the generated signals summing at the electron detector. Many attempts to control electron beam penetration and its effects in the SEM on the signal generated have been attempted over the years. [2,3,4,5] However, one of the major, and most successful, approaches to lessen the electron beam penetration has been employing low landing energy focused electron beams.[†]

1.1 Low Landing Energy. Low accelerating voltage scanning electron microscope (LVSEM) inspection and characterization has been done since the early work in this field by workers such as Zworykin, Hillier and Snyder.[6] However, this early work suffered from problems of poor spatial resolution, due to lack of excellent focusing ability of the simple electron-optical column and the type of electron sources (tungsten filaments), poor signal-to-noise ratio (S/N), and inadequate detectors and amplification. More energetic and intense electron beams caused stronger sample charging and in oil-based vacuum systems resulted in significant surface contamination making it a difficult technique beyond academic research. These were the reasons why most pre-1980s SEM operation was done mostly on conductive samples or samples coated with a thin metal or carbon layer, and almost exclusively, at high landing energies. The late 1980s brought the advent of high-brightness cold field emission instrumentation and digital electronics. With those innovations, non-destructive [7], low accelerating voltage at or lower than 1 keV imaging and inspection became the norm for many industries, especially the semiconductor industry, and has been successful in this role for the past several decades placing LVSEM within high-volume industrial applications. The application of cold and then thermal field emission electron sources afforded far superior S/N with higher resolution than tungsten or lanthanum hexaboride electron sources. However, at low accelerating voltages, sample contamination remained a confounding issue since the lower landing energy primary electrons generate more secondary electrons at the sample surface, and low-energy secondary electrons are responsible for contamination deposition. With the advent of cleaner instruments and advanced sample cleaning procedures, eventually many of these issues were solved.[8]

1.2 Electron Beam Penetration. The electron beam, depending upon sample composition, landing energy and the angle of incidence, penetrates to a certain depth. An approximate penetration depth can be calculated with an equation developed by Kanaya and Okayama.[9] As shown in Figure 1, the approximate calculated range in Si is about 9 micrometers for a 30 keV landing energy beam and that decreases to about 30 nanometers for low accelerating voltage imaging at 1 keV and progresses closer to the surface at lower landing energies. This has immense influence on the imaging and effects of charging [10] and why it has been so successful in non-destructive imaging for semiconductor manufacturing. However, the values obtained by this equation may be unreliable at the lowest landing energies because the Kanaya/Okayama model was developed long before the application of LVSEM or for that matter ULVSEM. More recent modeling incorporates more modern equations for beam penetration, however more fundamental research needs to be done in this area to accurately understand these effects.

1.3 Information Volume. The information volume is the area where the acquired signal generated by the primary electron beam originates. It results from the primary beam size, and shape and depends on the landing energy and the trajectory of the primary electron beam and the sample material. Thus, the information volume can vary greatly. For x-rays in light, bulk materials this could be many cubic micrometers (μm^3), conversely for secondary electrons it could be close to 1 nm^3. The information volume is where any signal useful for the SEM originates. Although it must be understood that not all signal electrons have enough energy to leave the surface and be collected. The information volume is defined by the penetration depth, the spread of the electrons within the sample and the escape depth. Typically, the escape depth is the depth of the information volume, unless sample contrast based on charging is observable. [2]

[†] Low landing energy is generally synonymous with low accelerating voltage but is now used when dealing with some of the newer instrument models, such as the instruments used in this study. The primary difference is that in all those instruments the electron source can emit electrons at high accelerating voltage, but in many of the newer models the primary beam electrons can be decelerated to a lower landing energy in the column via electrostatic lenses and/or at the sample stage through biasing. This technique allows the electron optical column to operate more optimally and provide higher spatial resolution.

Figure 2 shows the results of a Monte Carlo simulation [11] of 500 electrons for a primary electron beam having a fixed 0.5 nm in diameter. The electron trajectories in silicon (Si) and the gold (Au) samples are very different at 30 keV and 1 keV landing energies. The yellow to blue colors indicate the decreasing energy of the electrons in the sample, and the red trajectories denote backscattered electrons. At 30 keV landing energy, a large number of signal electrons‡ are generated and escape at the incident spot's location, thus making excellent spatial resolution possible, even when there are electrons, as shown, escaping remotely from that spot. Those electrons escaping remotely do not carry high spatial resolution information; essentially, they result in only a background. This background typically varies little over small details and slowly over much larger dimensions than the well-focused primary electron beam. The same is true for secondary electrons generated deeply in the sample, except many of them do not possess enough energy to become signal.

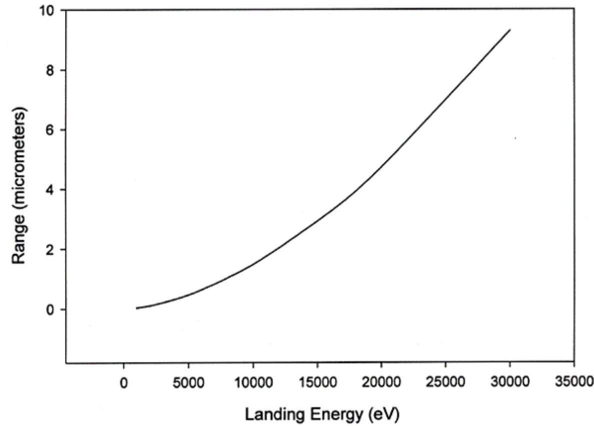

Figure 1. Approximate range of the calculated electron penetration in silicon from 1 keV to 30 keV landing energies.

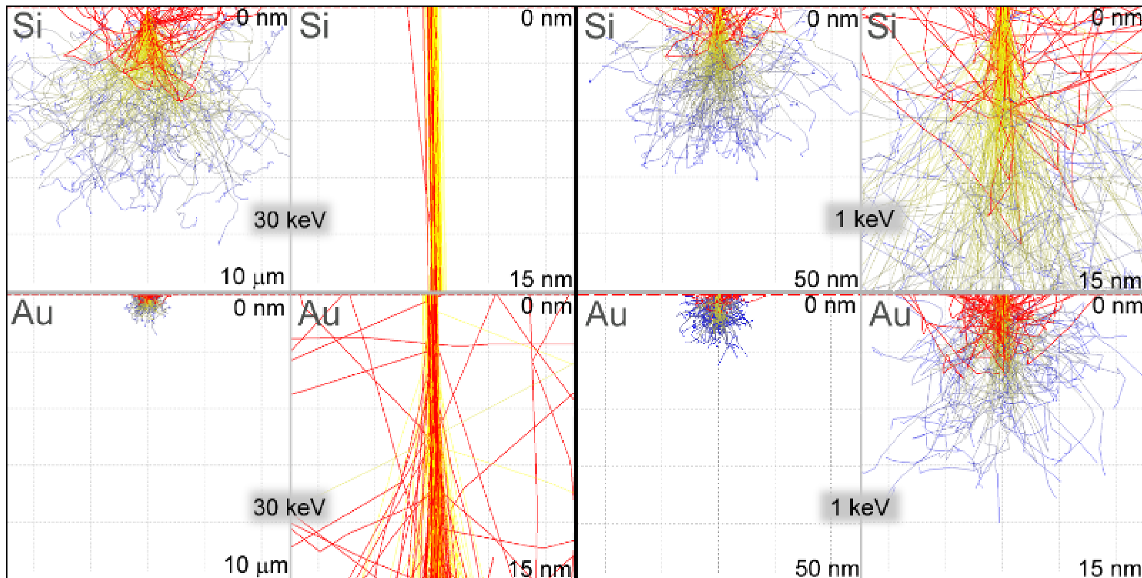

Figure 2. Monte Carlo simulated trajectories for Si (the upper 4) and for Au (the lower 4 results) (right). The scale for 30 keV is 10 μm and for 1 keV 25 nm and 15 nm for all magnified portions.

However, due to the very shallow escape depth of the secondary electrons, those generated within that region do carry information about the very top few nanometers of the sample. In the SEM in the secondary electron imaging mode, a single-layer of graphene can be readily distinguished from areas having 2, 3 or 4 layers.[12] A monoatomic layer of carbon, as graphene, on the top of a clean copper (Cu) sample significantly changes the intensity of the peak energy and energy

‡ Used here, signal refers to those electrons making up the image without discrimination to type.

distribution of secondary electrons.[13] At this point, the use of much lower landing energies to restrict the secondary escape depth below what traditional SEMs employed becomes very exciting. At these lower landing energies, it is possible to explore new untapped possibilities for new nanometer-scale measurements, such as the thickness of nanocoatings.

Over the evolution of SEM, obtaining more of the surface detail and minimizing sample damage became more important and as low landing energy techniques and instrumentation improved, the useful landing energy was decreased to sub-1 keV. Especially in integrated circuit production, 600 eV - 300 eV landing energy became widely used in combination of sample biasing, which has several advantages.[14] However, whenever accelerating voltages are reduced, noise increases due to the reduced apparent source brightness, making imaging difficult. For example, the apparent brightness (B) is a function of the accelerating voltage (Va):

$$B = Bc \cdot Va/Ve$$

where Bc is the source or cathode brightness and Ve is the effective emission voltage (energy) of the electrons leaving the source (electron gun). Bc depends on the source technology (nanotip, cold or heated field emission, tungsten, etc.). At low landing energies, B becomes overwhelming but the S/N of the generated signal actually improves, as more secondary electrons per incoming primary electron may emerge from a shallower excited volume (at high landing energies most of the secondary electrons die deep within the sample). What suffers is the focusing ability due to the dominant presence of chromatic aberration, which is the key problem with low-energy electrons when energy variation becomes a larger relative problem: 2 eV variation in 10000 eV beam is a much smaller portion than with 500 eV.

In general, it is not clear what happens at very low landing energies. Local sample surface potentials play a role as well as the surface geometry and the surface molecular and elemental composition. The penetration depth for metals is shallower. For non-conductive samples it is deeper and can be more than 10 nm. For secondary electron imaging the minimum is around 100 eV and is lower for metals. Under 50 eV the landing energies of primary electrons start to behave as "valence" electrons and get "smeared". This behavior contributes to reduced spatial resolution.

Digital electronics and the associated frame averaging methods have improved the limitations of LVSEM. In addition, newer SEM designs, employ clever lens designs with through-the-lens electron detection improved the image sharpness greatly due to shorter final lens focal lengths (even for large samples). In addition, modern lens designs incorporating through-the-lens electron detection afforded better electron collection efficiency and the ability to use multiple detectors within short working distances. All of these factors together are critical to the success of LVSEM. However, S/N and chromatic and spherical aberrations remain significant.

1.4 Ultra-Low Landing Energy and Beam Deceleration. Classically, the emitted electrons leaving the electron gun, attain an energy value close to the applied accelerating voltage and then travel down toward ground potential through the electron optical column to impinge on the sample. High accelerating voltage electron sources have higher apparent brightness, shorter wavelengths and reduced spherical and chromatic aberrations than those emitted at lower accelerating voltage. ULVSEM utilizes all of the above instrument improvements applied to LVSEM and builds upon it by relying upon the advantages provided by a high accelerating voltage electron beam. A beam of high-energy electrons travels down the column and is decelerated just before it reaches the sample. If the beam is decelerated within the column by methods such as: electrostatic decelerating lens design (Figures 3a and b) and/or an applied sample bias, the primary electron beam impinges on the sample with a landing energy much less than the initial accelerating voltage at the electron source. But through this deceleration, the beam cleverly retains most of the advantages afforded to higher accelerating voltage applications including high-brightness and lower spherical and chromatic aberrations while landing at the decelerated, ultra-low voltage chosen.

1.5 Effects of Electron Beam Penetration. Classical secondary electron escape depth is 2 to 5 nm for metals, and potentially deeper than 10 nm for insulators. Therefore, all electrons collected, resulting from a landing energy of 50 eV or lower, are secondary electrons by definition. Below 100 eV landing energies the penetration depth, the depth of the information volume, the inelastic mean free path (IMFP) of the electrons are no longer diminishing with diminishing beam energy, the IMFP can, rather. increase [15] Also, according to current work, under 100 eV landing energies the SE yield does not increase, it can actually decrease. According to Powell [16] for Cu the IMFP is the smallest, about 0.5 nm at around 80 eV then it goes up and reaches over 1 nm at 10 eV. Therefore, for ULVSEM operation it is especially important

to optimize the landing energy to obtain the best results. This underscores the need for further modeling and simulation for very low energy SEM imaging and measurements for them to be suitably accurate for practical use.

1.6 Nanoengineering Applications. Nanoparticle and critical dimension metrology in the research environment currently relies on measurement of the collected secondary electron data. For novel materials manufactured for nanoengineering applications, these data are essential to appropriately analyze compositional and morphological characteristics of products and ULVSEM presents a new technique to obtain this information. Both scanning electron and transmission electron microscopy are excellent tools for this. For example, manufactured soft materials for biomedical applications typically have dimensions of less than 100 nm. The class of nanocellulose-based materials for the biosciences is another good example. Cellulose has a long history of applications in the pharmaceutical industry. Recently, nanocellulose has been successfully studied by LVSEM and now ULVSEM can also be applied to these novel materials.

In addition, the dimensions of nanogels are on the order of nanometers, generally less than 100 nm though larger gels are possible. Nanogels require advanced dimensional metrology efforts to fully understand the size and shape of the materials. Both scanning electron and transmission electron microscopy are excellent tools to better understand these manufactured soft materials. Commercially available ionic liquids [17, 18, 19, 20, 21] have been an ideal approach to improve the contrast of these types of materials and offer the ability to keep the materials in their hydrated state. The visualization of specimens in a hydrated/wet state is a key factor for many applications in electron microscopy to appropriately analyze compositional and morphological characteristics. For these materials, sample charging is one of the typical problems encountered in investigating these insulating samples. Traditionally utilized metal coating of the sample surface is not very useful, as the charge suppression is not satisfactory or important fine details of the sample get obscured. Commercial ionic liquids have offered an additional technique for the preparation of these samples, however ULVSEM now provides and additional technique to understand surface interactions and structural details. Coupling ultra-low landing energy and beam deceleration with these types of sample preparations will be something in the future as soft matter manufacturing continues to grow along with the needs for better contrast capabilities for materials in a hydrated state. Soft matter, such as polymer hydrogels, which consist of three-dimensional polymer networks of soft, gelled particles in water, or nanocrystalline cellulose, which exhibits promising mechanical properties and good biocompatibility is an excellent candidate class of materials for the application of ULVSEM.

2. MATERIALS AND METHODS

2.1 Instrument. The instrument used for the ultra-low accelerating voltage experiments was a Hitachi SU7000 field emission scanning electron microscope with a Schottky thermionic emission source (Figure 3a) or a Hitachi Regulus8230 cold field emission instrument. The SU7000 instrument has two condenser lenses and the final condenser lens of the instrument constructed with a novel, combined, field-free electrostatic, and electromagnetic lens (Figure 3b). The final lens acts: 1) to finely focus the electrons electromagnetically, and 2) to electrostatically decelerate them. The electrostatic lens acts independently against the accelerating voltage, to decelerate the electron beam. The beam travels through the upper column at a high accelerating voltage, which is then influenced by a positive bias voltage (Vb) applied to the beam. The beam is then effectively decelerated to the required landing energy at the lower end of the column and ultimately interacts with the sample. The Regulus8230 instrument has a sample stage incorporating stage biasing capabilities.

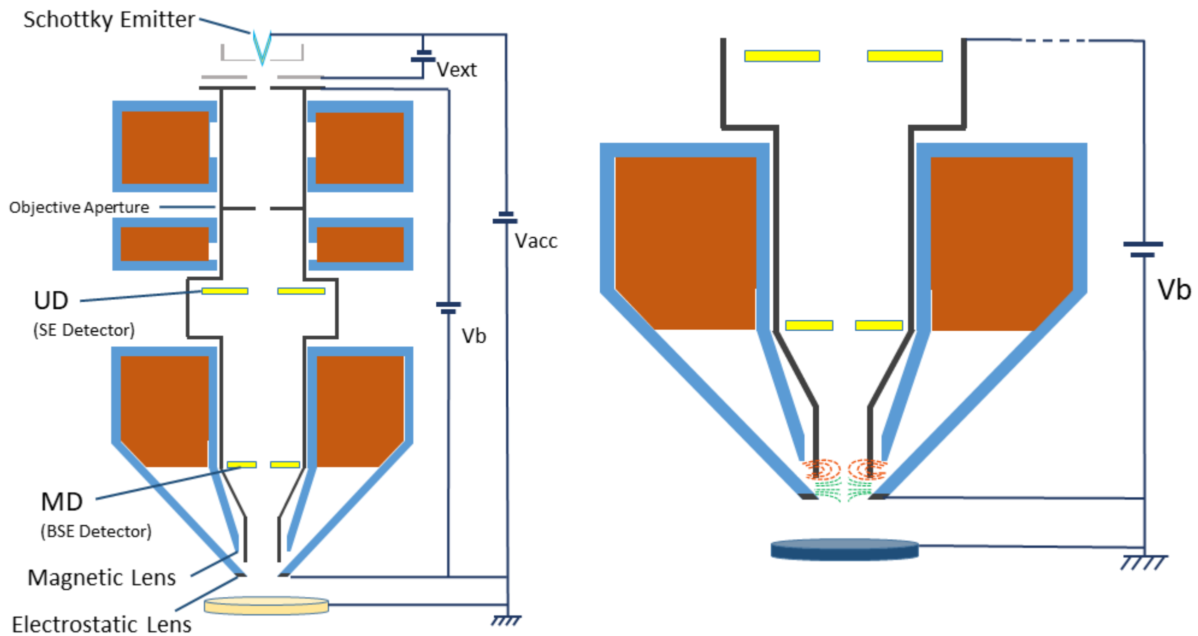

Figure 3. (a) Diagrammatic representation of the electron optical column showing the electron emitter, and lenses. (b) Diagram of the final lens of the instrument showing the electrostatic and electromagnetic components.

2.2 Electron Detectors. The instrument was equipped with multiple electron detectors (used depending upon application) both within the column and specimen chamber (see Figure 4). For the ultra-low landing energy work described here, the in-column, upper secondary electron detector (UD) was used for image collection for the examples provided.

- **Specimen Chamber Detectors.** Electrons emitted by the electron beam interaction with the sample at a low angle are collected "normally" in the specimen chamber by a lower, Everhart-Thornley type detector (LD). An ultra-variable pressure detector (UVD) may also be in the specimen chamber to collect the cathodoluminescence/secondary electrons emitted in high pressure operation, a typical solid-state diode backscattered electron detector (PDBSED) was also present.
  In-Column Detectors. Electrons emitted with a high trajectory by the primary electron beam interaction are accelerated toward the inside of the column by the electrostatic field. This field separates the electrons according to their energy. High up in the column, the upper detector (UD), typically collects secondary electrons spiraling back up the column with a small mix of backscattered electrons, and the middle-detector (MD) collects the high-angle backscattered electrons.

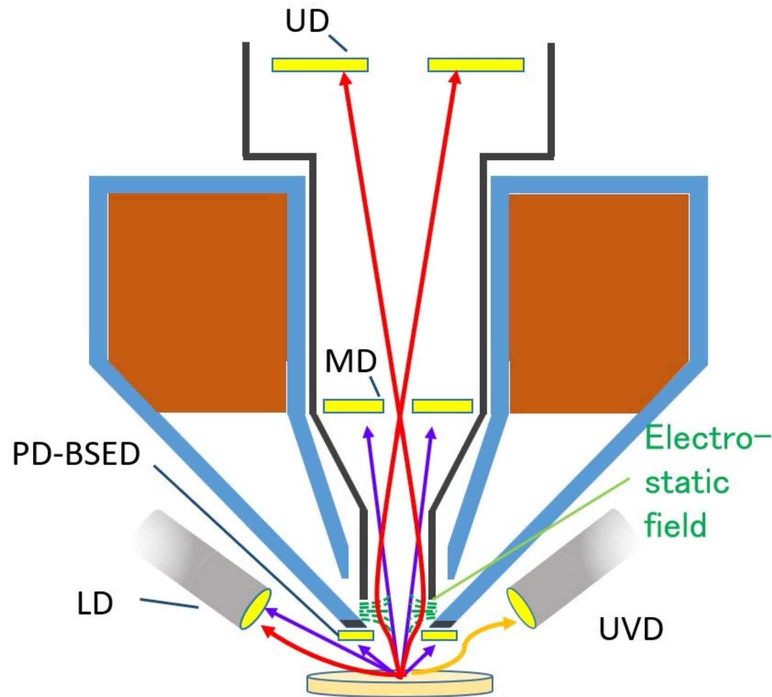

Figure 4. Diagrammatic representation of the positions of the multiple detectors as described in the text.

3.0 RESULTS

A comparison of two images of an electrode taken using beam deceleration in a ULVSEM is shown in Figure 5. Figure 5a shows an image of the surface of an electrode viewed at low landing energy (1 keV). Although this appears similar to a LVSEM, this image is not be typical of current state of the art SEM imaging at low landing energies. This is much improved since it is much sharper resulting from the beam deceleration effects. If the image were re-taken with standard LVSEM conditions at 1 keV it would not be as sharp due to lower S/N and the effects of spherical and chromatic aberrations. The range of the primary beam electrons under these conditions would be approximately 3 nm or about 3 times the secondary electron escape depth. Note the edge brightening characteristic displayed typical of the secondary electron image, this edge brightening leads to uncertainty in the edge locations and measurement of the nanometer sized particles present in the image. These nanometer sized particles can be precisely measured, but that the edge brightening leads to uncertainty in the measurements which could be minimized by modeling.[17, 18] Figure 5b shows an ULVSEM (10 eV) image. Note that the image appears flat because of the lack of edge enhancement effect, i.e., at 10 eV landing energy the depth of the information volume very small. The few 10 nanometer size objects shown in the digitally magnified inset are now revealed to be particles sitting on the surface of the sample. In the 1 keV landing energy image, these particles appear as small holes of the sample surface.

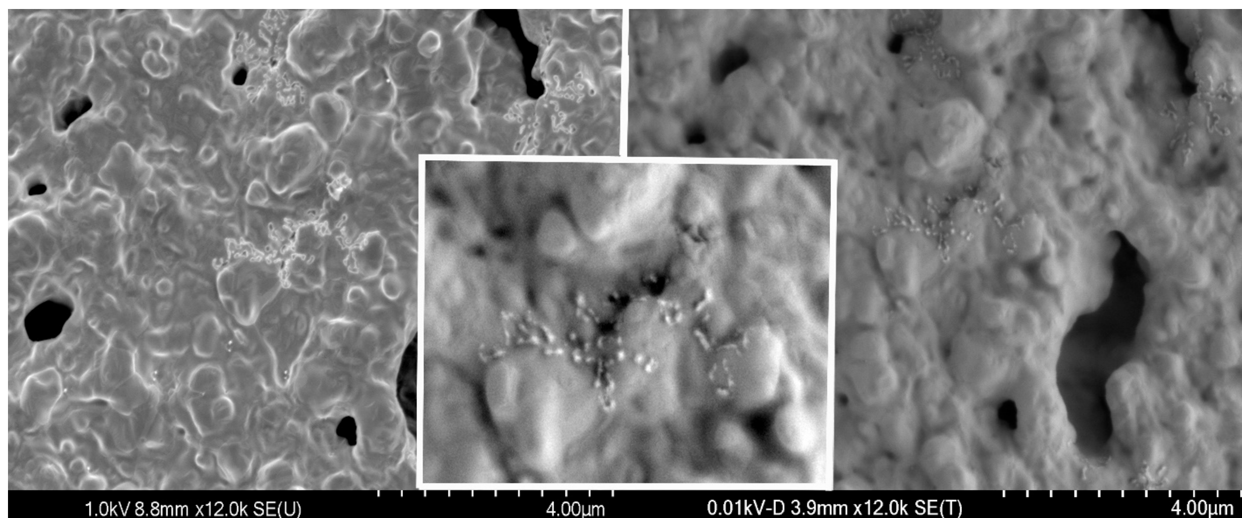

Figure 5. Surface of an electrode viewed at low landing energy, 1 keV (left) and ultra-low landing energy, 10 eV (right). The horizontal field width (HFW) is 10.5 µm for both images. The inset in the center is a digitally enlarged area (HFW 6.8 µm) revealing small sample features of about 40 nm.

4. CONCLUSIONS

Ultra-low accelerating voltage or ultra-low landing energy scanning electron microscopy (ULVSEM) is a new and exciting methodology being applied to thin films, nanocoatings, nanogels, nanofabrication, nanometrology, and nanoparticle analysis. Instrument conditions utilized in this mode are far different than contemporary SEM observation or even contemporary low accelerating voltage (LVSEM) imaging. Using this modality, the landing energy of the primary electron beam can be reduced to below 50 eV, even as low as 10 eV. Thus, as shown in this work, the electron beam penetration is reduced tremendously over previous methods and surface sensitivity is improved. Nanometer-scale details are enhanced, and secondary electron edge enhancement or "blooming" contributing to measurement uncertainty is greatly reduced, potentially leading to more precise metrology once this imaging mode is fully characterized and modeled. High-resolution field emission electron sources, improved lens, detector designs, and electron deceleration and/or sample biasing all contribute to the ability to image at such low energies. Ultra-low landing energy is clearly a new, exciting imaging and measurement working mode of the SEM, which will result in new scientific knowledge for nanometer-scale scientific and engineering applications.

5. REFERENCES

1. Postek, M. T., Vladár, A. E., "Does Your SEM Really Tell the Truth? How would you know? Part 1," SCANNING 35:355-361 (2013). https://doi.org/10.1117/12.2065235
2. Zhao, M. et al. New Insights into Subsurface Imaging of Carbon Nanotubes in Polymer Composites via Scanning Electron Microscopy. 2015 doi: 10.1088/0957-4484/26/8/085703.
3. Wells, O.C. (1971). Low-loss image for surface scanning electron microscope. Appl Phys Lett 19(7), https://doi.org/10.1063/1.1653899
4. Postek, M.T., Vladár, A.E., Wells, O.C. & Lowney, J.L. 2001. Application of the low-loss scanning electron microscope (SEM) image to integrated circuit technology. Part 1. Applications to accurate dimension measurements. Scanning 23(5), 298–304. https://doi.org/10.1002/sca.4950230502
5. Wells, O.C. (1986). Low-loss electron images of uncoated photoresist in the scanning electron microscope. Appl. Phys. Lett. 49(13), 764–766. https://doi.org/10.1063/1.97540
6. Zworykin, V. K., Hillier, J. and Snyder, R. L. 1942 A scanning electron microscope. ASTM Bulletin August 1942 15-23.
7. Postek, M. T. 1987. Non-destructive Submicron Dimensional Metrology using the Scanning Electron Microscope. Review of Progress in NDE 6(b):1327 1338. https://doi.org/10.1007/978-1-4613-1893-4_150

8. Postek, M. T., Vladár, A. E., Kavuri, P. P., "Does Your SEM Really Tell the Truth? How would you know? Part 2. Specimen Contamination" SCANNING 36:347-355 (2014). DOI: 10.1002/sca.21124
9. Kanaya, K and S. Okayama, S. 1972. Penetration and energy loss theory of electrons in solid targets. J. Phys. D: Appl. Phys. 5: 43- 58. doi: 0.1088/0022-3727/5/1/308
10. Postek, M. T., Vladár, A. E., 2015. Does Your SEM Really Tell the Truth? How Would You Know? Part 4. Charging and its mitigation. SPIE SCANNING Microscopy Vol. 9636. 1 – 12 doi: 10.1117/12.2195344
11. Casino Monte Carlo simulation of electron trajectories in solids. Université de Sherbrooke, Québec, Canada https://www.gel.usherbrooke.ca/casino/What.html
12. Lee L. H. et al. 2018 Plan-view Transmission Electron Microscopy Specimen Preparation for Atomic Layer Materials using a Focused Ion Beam Approach, J. Ultramicroscopy doi: 10.1016/j.ultramic.2018.12.001
13. Cao M. et al. 2017, Secondary electron emission of graphene-coated copper https://doi.org/10.1016/j.diamond.2016.09.019
14. Postek, M. T., Larrabee R. D., and Keery W. J. 1989. Specimen Biasing to Enhance or Suppress Secondary Electron Emission from Charging Specimens at Low Accelerating Voltages. SCANNING 11:111 121. https://doi.org/10.1002/sca.4950110302
15. Yu, O. et al. 2020 Low energy (1–100 eV) electron inelastic mean free path (IMFP) values determined from analysis of secondary electron yields (SEY) in the incident energy range of 0.1–10 keV, https://doi.org/10.1016/j.elspec.2019.02.003
16. Powell, C. J. 2019, Practical guide for inelastic mean free paths, effective attenuation lengths, mean escape depths, and information depths in x-ray photoelectron spectroscopy, https://doi.org/10.1116/1.5141079
17. Kilcrease, J. P. and Voelkl, E., "Liquid in-situ transmission electron tomography using Hitachi HILEM IL1000 ionic liquid," Microscopy and Microanalysis, 22(Suppl 3), 810-811 (2016) https://doi.org/10.1017/S1431927616004906.
18. Kilcrease, J. P., Takagi, O., Bauchan, G., "Correlative light and electron microscopy (CLEM) utilizing Hitachi HILEM IL1000 ionic liquid", Microscopy and Microanalysis 22(Suppl 3), 246-247 (2016) https://doi.org/10.1017/S1431927616002087.
19. Muto, A., Shibata, M., Konomi, M., Yasuda, R., and Kamasawa, N., "Correlative Fluorescence and Scanning Electron Microscope Imaging of Cultured Neurons Pretreated with Ionic Liquid," Microscopy and Microanalysis 22(Suppl 3), 232-233 (2016) https://doi.org/10.1017/S1431927616002014.
20. Sakaue, M., Shiono, M., Konomi, M., Tomizawa, J., Nakazawa, E., Kawai, K., Kuwabata, S., " New Preparation Method using Ionic Liquid for Fast and Reliable SEM Observation of Biological Specimens," Microscopy and Microanalysis 20(Suppl 3), 1012-1013 (2014) https://doi.org/10.1017/S1431927614006783.
21. Shiono, M., Sakaue, M., Konomi, M., Tomizawa J., Nakazawa, E., Kawai, K., and Kuwabata, S. "Ionic liquid preparation for sem observation of minute crustacean," Microscopy and Microanalysis 20(Suppl 3), 1016-1017 (2014) https://doi.org/10.1017/S1431927614006801.
22. Postek, M. T., Vladár, A. E. and Villarrubia, J. and Atsushi Muto. 2015. Comparison of Secondary, Backscattered and Low Loss Electron Collection for Dimensional Measurements in the SEM. Part 2. Proc. Microscopy Soc. of America https://doi.org/10.1017/S1431927615006315
23. Villarrubia, J.S., Vladár, A.E. & Postek, M.T. 2005. Scanning electron microscope dimensional metrology using a model-based library. Surf Interface Anal 37, 951–958. https://doi.org/10.1002/sia.2087